

Nature of Cation Mixing and Ordering in Na-Ca Silicate Glasses and Melts

Sung Keun Lee^{*,†} and Jonathan F. Stebbins[‡]*Geophysical Laboratory, Carnegie Institution of Washington, Washington D.C. 20015, and Department of Geological and Environmental Sciences, Stanford University, Stanford, California 94305-2115**Received: November 18, 2002; In Final Form: January 28, 2003*

Soda-lime silicate glass is the fundamental base glass for many technologically important oxide glasses, and it has been used as window glass since the Roman Empire. Mixed-cation silicates also are useful models of the structure and dynamics of basaltic magmas and mantle melts. The diffusivity of Na⁺ in silicate melts and its variation with composition play key roles in melting behavior. This property also depends strongly on the composition and framework structures of glasses and melts and on the presence of other types of nearby cations that often impede Na motion; this is known as a *mixed cation effect*. Structure-dependent silica activity also controls the composition of melts in equilibrium with mantle peridotite. Despite its importance, little is known about the detailed atomic structure and the degree of cation mixing in Ca-Na silicate glasses and melts with varying composition. Most modeling efforts assume a random distribution of these cations. Here, we use ¹⁷O magic angle spinning (MAS) and triple quantum magic angle spinning (3QMAS) NMR to show nonrandom distributions of the network-modifying cations Na and Ca in Ca-Na silicate glasses, by probing the atomic configurations around the nonbridging oxygens. Nonrandomness in Na–Ca mixing, in particular the prevalence of Na–Ca pairs in this system, was clearly observed in ¹⁷O MAS and 3QMAS NMR where several nonbridging oxygen peaks such as Na–O–^[4]Si, and mixed peaks ({Na,Ca}–O–^[4]Si) are partially resolved. The observed fractions of Na–O–^[4]Si are smaller than those predicted by random distributions of Na and Ca, suggesting preference to dissimilar pairs. There are also considerable interactions between bridging oxygens and charge-modifying cations, which supports rather homogeneous distribution of such cations. ²³Na MAS NMR spectra at high field (14.1 T) provide information on chemical shift distributions with relatively small perturbations from quadrupolar broadening and provide further support for significant Na–Ca mixing. The results given here partly account for reduced Na diffusion when mixed with Ca, and together with nonrandom distributions of nonbridging oxygens, lead to negative deviation in silica activity. This also contributes to atomistic models of several magmatic processes.

Introduction

The extent of cation mixing in mixed-cation silicate glasses and their precursor liquids has long been studied, because of the technical and scientific importance of these systems. The quantification of atomic disorder in silicate glasses is essential for understanding the microscopic origin of many transport and configurational thermodynamic properties, including silica activity and dynamic processes of silicate melts.^{1–5} Yet the details of atomic-scale disorder among nonframework cations such as Ca and Na in simple Ca-Na silicate glasses are far from being understood.

The nonframework cations perturb silicate frameworks linked by bridging oxygen (BO), by forming nonbridging oxygens (NBO), which play essential roles in many dynamic properties of melts. There are two key questions regarding the structure of mixed-cation silicate melts: To what extent are these cations distributed around BO and NBO, and what effect does this state of disorder have on the melt properties? Many experimental and theoretical previous studies on various mixed-cation silicate glasses have reported seemingly incompatible results, including random mixing between these cations with homogeneous

distribution of both charge balancing cations,⁶ random mixing of two types of cations with alkali segregation,^{7,8} chemical order favoring dissimilar pairs,⁹ and clustering of similar cations,¹⁰ depending on the types of cations and experimental and theoretical methods used. The types of cations in oxide glasses certainly can cause different states of disorder depending both on their characteristics, such as ionic radius and charge, and on their local environments; however, some of these discrepancies may originate from the model dependence of the analyses and the fact that clear and direct experimental evidence has been quite limited. Quantifying this atomic disorder could help to explain many interesting material properties related to the mixed-cation effect, where the presence of other cations may strongly inhibit ionic diffusion.^{11,12}

Randomness in many disordered systems can be better quantified by probing the local environment around oxygens such as NBO and BO, as was recently demonstrated in several oxide glass systems.^{13–16} A pioneering ¹⁷O magic angle spinning (MAS) NMR study on CaSiO₃–MgSiO₃ glasses showed that NBO sites indeed reflected the compositional variation, with clear existence of a mixed NBO peak (e.g., {Ca,Mg}–O–Si). This supports extensive mixing among Ca²⁺ and Mg²⁺ around NBO. Two-dimensional NMR techniques such as DAS (dynamic angle scattering)¹⁷ and 3Q (triple quantum) MAS NMR yield better resolution, free from residual anisotropic line broadening due to second-order quadrupolar interaction,¹⁸ and

* To whom correspondence should be addressed: phone, (202) 478-8968; e-mail, s.lee@gl.ciw.edu.

[†] Carnegie Institution of Washington.

[‡] Stanford University.

have provided improved prospects for understanding cation disorder in mixed-cation silicate glasses such as K-Mg silicate,¹⁴ K-Na disilicates,¹⁵ and Ca-Ba silicate glasses.¹⁶ These results of considerable mixing are also roughly consistent with the results from Kirkpatrick¹³ while the K-Mg system shows greater ordering and the K-Na and Ca-Ba systems can be described by random mixing of the cations. On the other hand, the quantitative assessment of the extent of disorder had been hampered due to overlap among NBO peaks, thus making results rather model dependent. Ca-Na mixed silicate glasses are one of the ideal systems for exploring the extent of mixing among cations because of the difference in cation field strength and a relatively large chemical shift difference between Ca-NBO (Ca—O—^[4]Si) and Na-NBO (Na—O—^[4]Si).¹⁹ In addition, Na-NBO has a distinct and narrow chemical shift range that can be used as a probe of the degree of intermixing among cations.¹⁹

In charge-balanced aluminosilicates (a model system for rhyolitic magmas) or in binary borosilicate glasses²⁰ with low fractions of NBO, nonrandomness stems mostly from partial ordering of the framework. This has been recently quantified with a general model for the extent of intermixing among framework cations (^[4]Si, ^[3]B, and ^[4]Al) in aluminosilicate and borosilicate glasses, using ¹⁷O 3QMAS NMR to introduce the concept of *degree of Al avoidance and degree of phase separation*.^{4,5,21,22} These framework cations certainly deviate from random distributions in aluminosilicates, but they also violate the Al avoidance rule in that they display noticeable fractions of ^[4]Al—O—^[4]Al with some preference for forming ^[4]Si—O—^[4]Al. The degree of intermixing among framework units, together with possible nonframework disorder in oxide melts, can contribute significantly to the total negative or positive deviation of silica activity in silicate melts, as well as to the variation of Na diffusivity when mixed with Ca.^{5,8,23}

Here, we report the ¹⁷O MAS and 3QMAS spectra at two static magnetic fields (9.4 and 14.1 T) for a series of Ca-Na silicate glasses, with the aims of quantifying the degree of intermixing among cations, providing an atomic explanation of the dependence of silicate melt properties (thermodynamic and transport) on Na, and understanding composition-dependent melting relations in these systems. We finally discuss the structure of mixed cation glasses in general.

Experiments

Sample Preparation. Mixed silicate glasses with 75 mol % SiO₂ and Ca/Na ratio ($X_{\text{CaO}} = \text{CaO}/(\text{CaO} + \text{Na}_2\text{O})$) of 0 (NS13), 0.25 (CNS051560), 0.5 (CNS116), and 0.75 (CNS150560) were synthesized from carbonates (CaCO₃, Na₂CO₃) and ¹⁷O-enriched silicon dioxide prepared by hydrolyzing silicon tetrachloride in 46% ¹⁷O-enriched water. To avoid phase separation, a Ca end member with a somewhat lower silica content (CaO:SiO₂ = 38.5:61.5 mol %, CS46) was also synthesized. The mixtures were fused for an hour at between 1473 and 1913 K (depending on their melting temperatures) in an Ar atmosphere to prevent isotope exchange and then quenched. Negligible weight losses beyond those expected from decarbonation were observed during synthesis.

NMR Spectroscopy. ¹⁷O MAS and 3QMAS NMR spectra for Ca-Na silicate glasses were collected at two static magnetic fields on a modified Varian-VXR/Unity400 spectrometer (9.4 T) at a Larmor frequency of 54.22 MHz using a 5 mm Doty Scientific, Inc., probe and on a Varian Inova 600 spectrometer (14.1 T) at 81.07 MHz with a 3.2 mm Varian/Chemagnetics T3 probe. Recycle delays for ¹⁷O MAS NMR were 1 s with radio frequency pulse lengths of 0.3–0.35 ms (9.4 T) and 0.25

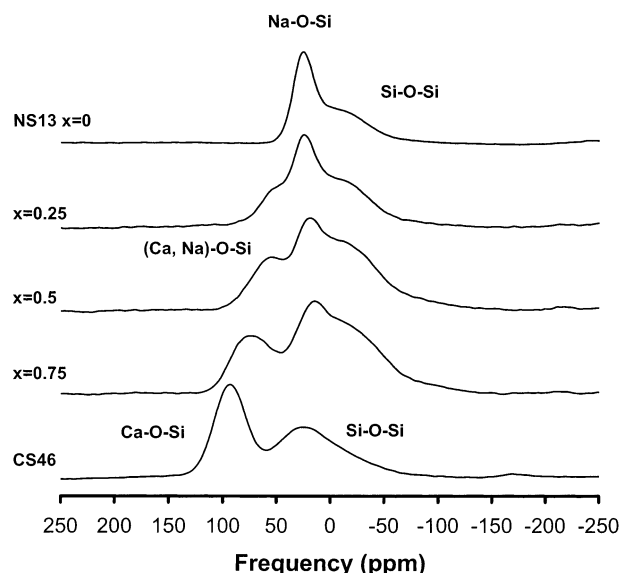


Figure 1. ¹⁷O MAS spectra for (CaO)_x(Na₂O)_{1-x}·3SiO₂ ternary glasses at 9.4 T.

ms (14.1 T) which corresponds to about a 15° tip angle for the central transition in solids. Sample spinning speeds of 15 and 18 kHz were used at the two fields.

In the 3QMAS NMR experiment at 9.4 T, the FAM (fast amplitude modulation)-based shifted-echo pulse sequence^{24–26} was used, comprising two hard pulses of duration 5.2–5.8 and 1.7 ms, and a soft pulse with duration of 26 ms and an echo time of about 0.5 ms, with recycle delays ranging from 1 to 10 s depending on the spin lattice relaxation time. ¹⁷O 3QMAS NMR spectra at 14.1 T were collected using a similar pulse sequence with hard pulses (3.0 and 0.7 ms) and a selective pulse with duration of 20 ms. The spectra are referenced to tap water (9.4 T) and ¹⁷O-enriched water (14.1 T). There was no significant difference in the resonant frequencies of the two standards.

²³Na MAS NMR spectra were collected with a Varian Inova 600 spectrometer at 14.1 T at 159 MHz, with a recycle delay of 0.1 s, a radio frequency pulse length of 0.2 ms, and spinning speed of 18 kHz. All spectra are referenced to 1 M NaCl solution.

Results

¹⁷O MAS NMR at 9.4 and 14.1 T. Figure 1 shows ¹⁷O MAS NMR spectra of the Ca-Na silicate glasses (CaO)_x(Na₂O)_{1-x}·3SiO₂ at 9.4 T with varying $X_{\text{CaO}} = \text{CaO}/(\text{CaO} + \text{Na}_2\text{O})$ and of CS46. Three main types of nonbridging oxygen are partially resolved: Na-NBO, Ca-NBO, and considerable fractions of {Na-, Ca}-NBO. Bridging oxygen (^[4]Si—O—^[4]Si) is also partially resolved. Na-NBO (NBO coordinated by three or four Na and silicon, Na—O—^[4]Si) is more shielded (peak at about 25 ppm) than Ca-NBO (peak maximum at about 100 ppm, Ca—O—^[4]Si). On the other hand, the chemical shift distribution of NBO in NS13 is less than that of Ca-NBO in CS46 glass, indicating increased number of possible configurations around Ca-NBO. In glasses with intermediate compositions, there is a wide distribution of chemical shift of NBOs between Na-NBO and Ca-NBO. The peak position of the mixed NBO peaks ({Na-, Ca}-O—^[4]Si) moves toward higher frequency (more positive peak position in MAS NMR spectra) with increasing Ca content. These results clearly indicate that there is extensive mixing of Ca and Na around NBO in mixed silicate glasses. The total

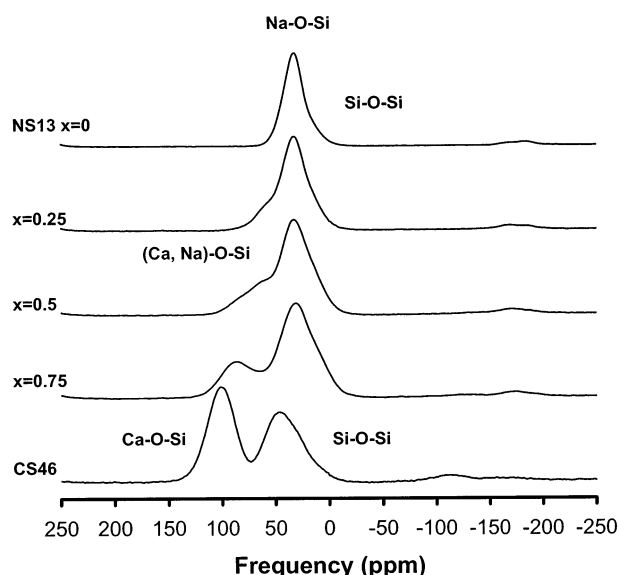


Figure 2. ^{17}O MAS spectra for Ca-Na silicate glasses at 14.1 T.

NBO peaks are broadest (largest chemical shift distribution) in the intermediate composition, implying that Na–Ca distribution around NBO shows neither complete preference for Na–Ca pairs nor significant clustering into Ca- and Na-rich regions (which would not allow large fractions of mixed peaks).

The bridging oxygen (BO) peak is also more deshielded in the Ca end member, which indicates that there are interactions between network-modifying cations and the bridging oxygen network. The variation of peak position for BO with different modifying cations is less than that of NBO. This result is roughly consistent with the perturbed modifying-cation distribution model, where the charge-modifying or balancing cations are homogeneously distributed with low probability of forming segregated channels but where they certainly show the specific preference for the framework with more net negative charge²⁷ (see Discussion). On the other hand, the larger difference in the NMR characteristics between the spectrum for CS46 and those of the others is also partly attributable to a different total network modifying cation content.

NMR spectra at multiple fields can provide better constraints on peak assignment and quantification. Figure 2 illustrates ^{17}O MAS NMR spectra at a higher field (14.1 T), where second-order quadrupolar broadening is reduced. The reduction of peak widths for the NBOs appears to be small because of their relatively small quadrupolar coupling constants (C_q) of about 2 MHz. This suggests that the peak widths in ^{17}O NMR spectra at 9.4 T mainly reflect the chemical shift distributions. On the other hand, peaks for BOs with larger C_q of about 5 MHz are greatly reduced in width at 14.1 T, and thus the peak overlap with Na–NBO increases. The overall information in these spectra is similar to that at 9.4 T, in that the chemical shielding of the mixed cation peaks increases with increasing Ca content because of greater dispersion of chemical shift in the intermediate compositions. In addition, the fraction of the Na–O– $^{[4]}\text{Si}$ peak around 25 ppm decreases with increasing Ca content. This site fraction is useful for quantifying the extent of intermixing between Ca and Na, as well as the relative preference of NBO between Na and Ca. On the other hand, there is overlap between Na–NBO and $^{[4]}\text{Si}$ –O– $^{[4]}\text{Si}$ as well as several mixed cation peaks in the ^{17}O MAS NMR spectra at both fields. ^{17}O 3QMAS NMR spectra can provide better resolution among peaks, as has been demonstrated in binary silicates and ternary aluminosilicate glasses.^{5,21,22}

^{17}O 3QMAS NMR at 9.4 and 14.1 T. Figure 3 shows the ^{17}O 3QMAS NMR spectra of Ca–Na glasses with varying Na/Ca at 9.4 T, where better resolution among the peaks for each type of BO and NBO is achieved.²⁸ Na–NBO has less chemical shift dispersion than Ca–NBO (in the isotropic dimension), suggesting that the Na configuration around NBO is more ordered than that of Ca–O– $^{[4]}\text{Si}$. This distinct and narrow chemical shift distribution of Na–O– $^{[4]}\text{Si}$ clearly separates it from other mixed cation NBO peaks, whose peak maxima move toward lower frequency (more negative in 3QMAS dimension) with increasing Ca content, consistent with the MAS NMR. Chemical shift dispersion of $^{[4]}\text{Si}$ –O– $^{[4]}\text{Si}$ also apparently increases. For structurally relevant NMR parameters such as quadrupolar coupling product, P_q (equal to $C_q(1 + \eta^2/3)^{1/2}$, where $0 \leq \eta \leq 1$ is the quadrupolar asymmetry parameter, C_q is the quadrupolar coupling constant), and the isotropic chemical shift (δ_{iso}), mean values can be estimated for each NBO and BO from the positions of the mixed peaks and from the centers of gravity for the end member peaks.^{18,29} The ^{17}O δ_{iso} and P_q of Na–O– $^{[4]}\text{Si}$ appear to be rather constant with varying Ca content, centered at around 36 ppm (± 1.5) and 2 MHz (± 0.15). Ca–O–Si in CS46 is more deshielded (δ_{iso} of 104.7 ± 2 ppm) and P_q is 2.2 MHz. The mixed NBO peak shows the most prominent variation with Ca content. The δ_{iso} and P_q of each mixed peak obtained from the positions of peak maxima are 60.3 ppm (1.6 MHz for CNS051560), 66.9 ppm (2.3 MHz, CNS116), and 93 ppm (2.4 MHz, CNS150560), respectively, indicating stronger interaction of charge-modifying cations with NBO than with BO, also consistent with the MAS NMR spectra. The ^{17}O δ_{iso} and P_q of $^{[4]}\text{Si}$ –O– $^{[4]}\text{Si}$ in NS13, obtained from the center of gravity of the peak, are about 52.8 (± 2) ppm and 4.6 (± 0.2) MHz, while those of CS46 are about 62.7 ppm and 4.3 MHz. The value of ^{17}O C_q has often been positively correlated to the $^{[4]}\text{Si}$ –O– $^{[4]}\text{Si}$ bond angle.³⁰ The trend seen here for BO sites in the end members may suggest that the average $^{[4]}\text{Si}$ –O– $^{[4]}\text{Si}$ angle in CS46 is narrower than that of $^{[4]}\text{Si}$ –O– $^{[4]}\text{Si}$ in Na silicates.¹⁴ The trend shown for P_q may also be affected by different total content of charge-balancing cations.

The relative populations of NBO and BO is not quantitative because 3QMAS efficiency depends on C_q .^{31,32} However, those of NBO are more directly comparable due to the similar C_q range for each type of NBO site.²² (See below for further discussion.) BO populations, with higher C_q , are underestimated in ^{17}O 3QMAS NMR spectra at 9.4 T with the radio frequency (rf) field strength of the experiment (about 70 kHz). On the other hand, the ^{17}O 3QMAS NMR spectra for Ca–Na silicate glass collected at 14.1 T with higher rf field strength (122 kHz) can provide better efficiency for larger C_q sites (BO). As shown in Figure 4, the chemical shift and its dispersion, as well as C_q of bridging oxygen sites are also variable with Ca/Na content, clearly indicating noticeable interaction between BO and charge-modifying cations. The chemical shift increases (decreases in 3QMAS dimension) with increasing Ca, and this trend is consistent with that of NBO. The C_q of BO also decreases with Ca. This is probably partly due to a larger mean bond angle distortion (narrowing) of $^{[4]}\text{Si}$ –O– $^{[4]}\text{Si}$ with the higher field strength cation. The $^{[4]}\text{Si}$ –O– $^{[4]}\text{Si}$ angles with smaller C_q values may thus be associated with Ca, again suggesting increased interaction between Ca and BO with increased Ca content. While the noticeable variation of NMR parameters of BO with X_{CaO} suggests considerable interaction between BO and network-

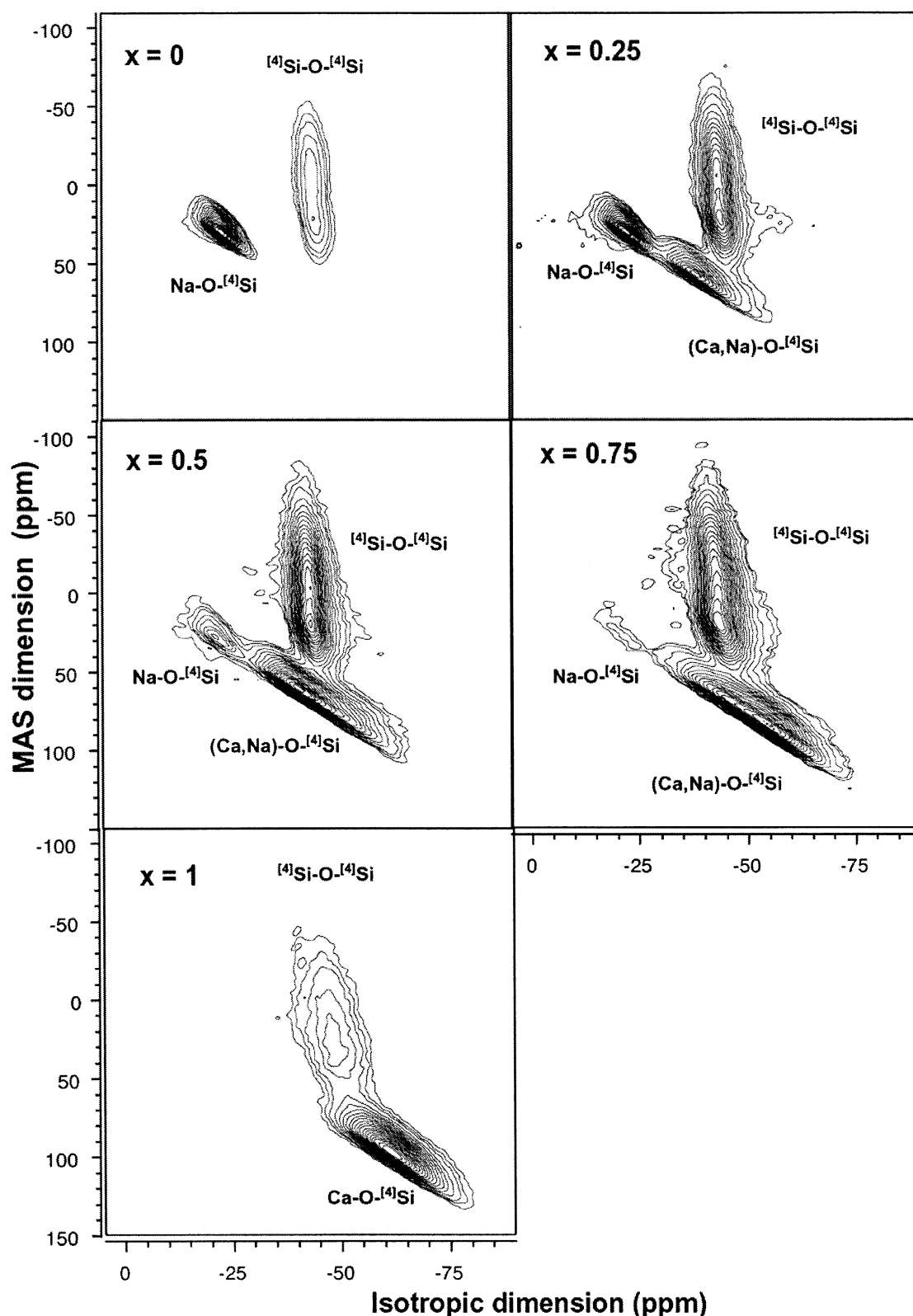


Figure 3. ^{17}O 3QMAS MAS spectra for Ca-Na silicate glasses at 9.4 T.

modifying cations, the detailed information on oxygen configurations around these cations still remains to be explored.

Figure 5 shows the total isotropic projections of the ^{17}O 3QMAS NMR spectra of CS46 and NS13 glasses. As discussed for the 2D spectra, Ca-NBO and Na-NBO have distinct chemical shift ranges, and Ca-NBO has a wider chemical shift distribution than Na-NBO. BO and NBO positions are also functions of Na/Ca, with NBO being more sensitive to the cation than BO.

The results all indicate that the melt structure, including framework topology of BO (e.g., $^{[4]}\text{Si}-\text{O}-^{[4]}\text{Si}$ angle), is clearly affected by types of modifying cations.²⁷

^{23}Na MAS NMR 14.1 T. A direct view of the Na environment using ^{23}Na NMR at “high field” can also be helpful to explore the sodium distribution in silicate glasses using the chemical shift distribution,²⁷ which is often correlated with Na-O distance and the size of the Na site.³³ The chemical shift

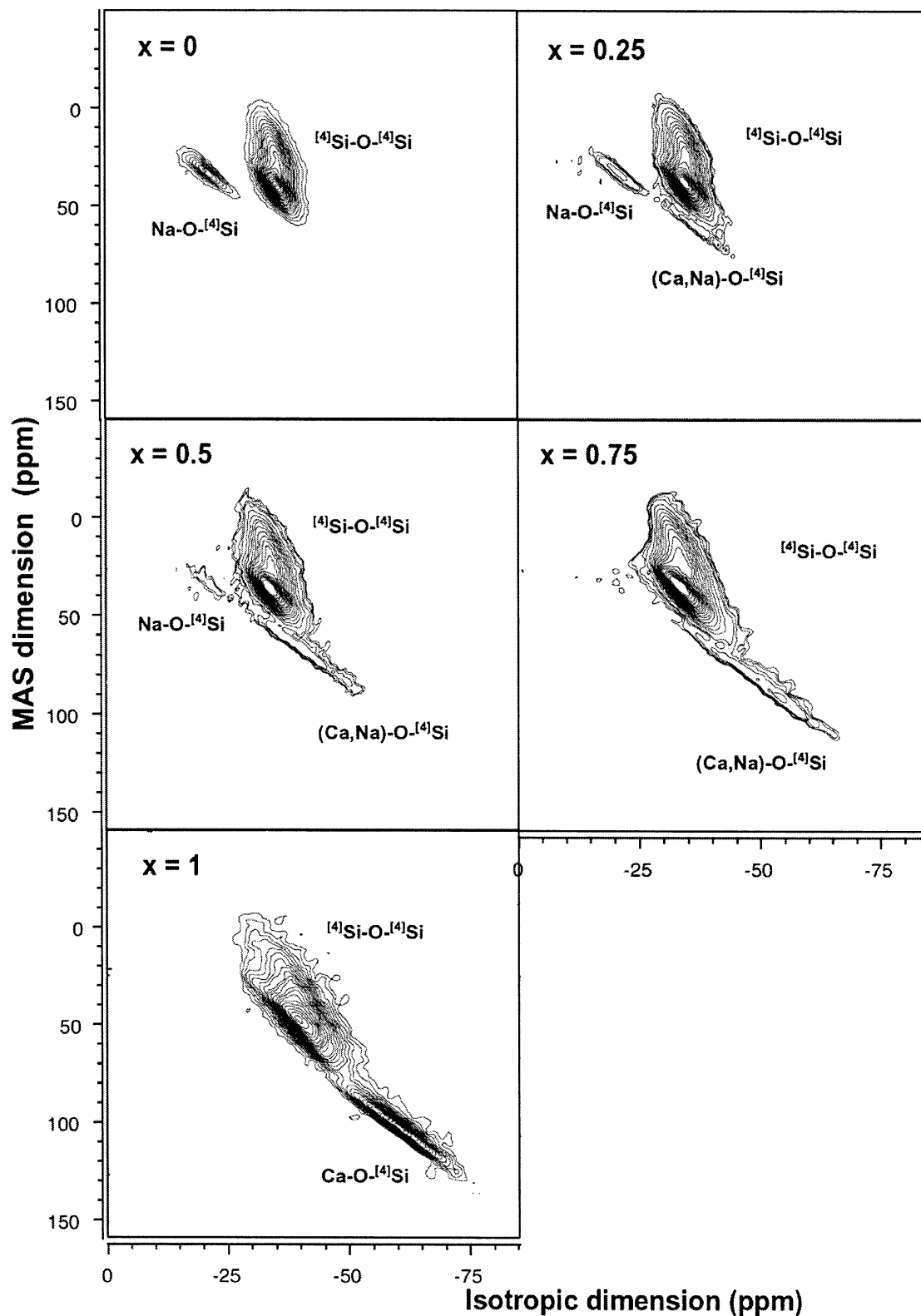


Figure 4. ^{17}O 3QMAS MAS spectra for Ca-Na silicate glasses at 14.1 T.

distribution is rather difficult to obtain from ^{23}Na MAS NMR spectra at lower field, but high field NMR can provide spectra where the quadrupolar broadening is effectively reduced and which thus yield information on isotropic chemical shift distribution.²⁷ Figure 6 shows the ^{23}Na MAS spectra of the Ca-Na silicate glass series. The peak maximum varies from -8.5 ppm (NS13) to about -14.7 ppm (CNS150560), which implies that average Na–O bond length or size of Na site slightly

increases from NS13 to CNS150560. This supports the hypothesis that there is structural rearrangement upon mixing. A similar correlation has been reported for mixed alkali silicate glasses, where addition of a larger cation appears to decrease the mean size of smaller cation sites and vice versa.³⁴ The ionic radii of Na and Ca are similar (Na^+ , 1.02 \AA ; Ca^{2+} , 0.99 \AA), and thus variation of Na–O distance here appears to be related to the effect of charge and medium-range order. For example, Na may

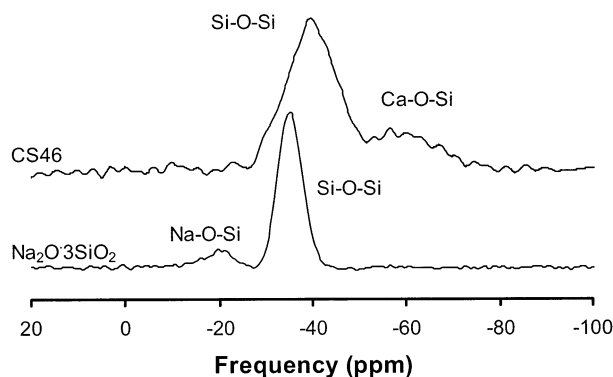


Figure 5. Isotropic projection of ^{17}O 3QMAS spectra for Ca-Na silicate at 14.1 T.

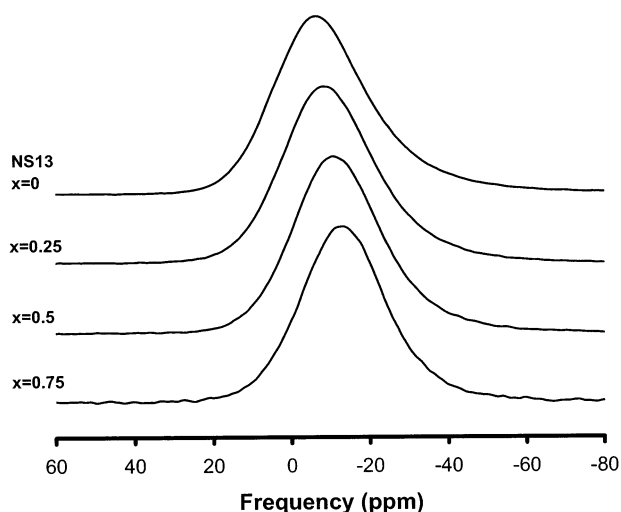


Figure 6. ^{23}Na MAS NMR spectra for Ca-Na silicate glasses at 14.1 T.

on average have a higher fraction of BO (vs NBO) in its first shell when Ca is present. The variation of ^{23}Na isotropic chemical shift may also stem from the variation of net negative charge on bridging and nonbridging oxygen upon mixing.²⁷

Also notable is that the full width at half-maximum (fwhm) of the ^{23}Na MAS NMR peaks are rather similar but increase slightly with increasing Na content, from 24.6 (± 0.5) ppm (CNS150560) to 27 (± 0.5) ppm (NS13). Because of the reduced second-order quadrupolar interaction (SQI) at this field, the peak width roughly represents the chemical shift distribution. The peaks for intermediate compositions are not broader but have intermediate values 25.9 (± 0.5) ppm (CNS116) and 26.7 (± 0.5) ppm (CNS051560). This trend suggests that Na and Ca are “uniformly” distributed, favoring dissimilar Ca–Na pairs; random distribution of Na and Ca would lead to wider fwhm for intermediate compositions.

Quantification of the Extent of Na–Ca Mixing. NBO Site Fraction. Oxygen site population analysis has been effective in quantifying the extent of intermixing among network cations.⁵ Here we analyze NBO populations from both 3QMAS and MAS NMR at 9.4 T. Because of uncertainty associated with the correct coordination number of NBO in mixed cation glasses, as well as a lack of direct information for the Ca end member (chemical shift of CS13 rather than CS46 here) and peak overlap, quantitative estimation of the population of each NBO peak in these glasses is not trivial. On the other hand, as shown in ^{17}O MAS and in particular 3QMAS spectra, the Na–O– ^{4}Si peak is clearly separated, and thus the fraction of Na–O–

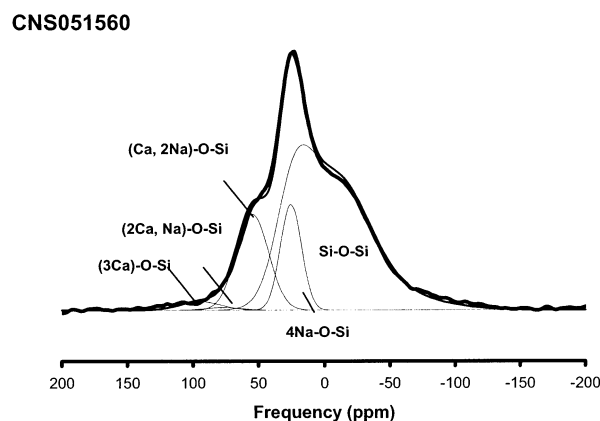
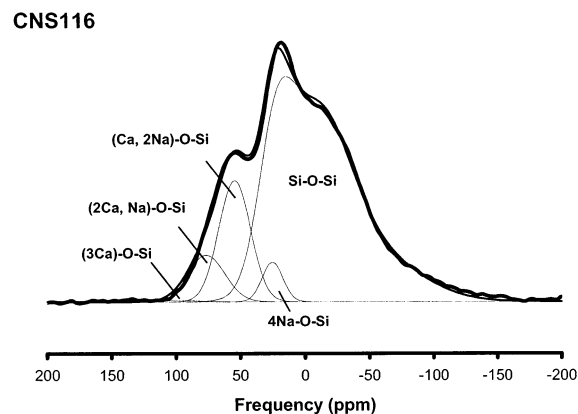


Figure 7. Fitting results of ^{17}O MAS NMR spectrum for CNS116 and CNS051560. Thick and thin lines refer to experimental and fitting results.

^{4}Si /total NBO is well constrained. In addition, the C_q values of all NBOs are similar at around 2 MHz, and their 3QMAS efficiencies should be similar as well.^{5,21} The Na–O– ^{4}Si /total NBO fractions were directly obtained from 3QMAS NMR by integrating the Na–O– ^{4}Si fraction in the 2D spectra and then fitting the MAS projection of the spectra (excluding Na–O–Si) with mixed NBO, Ca–O–Si, and BO peaks and directly comparing the fractions of NBO assuming equal 3QMAS efficiency. We also simulated the isotropic projection of the 2D NMR spectra with multiple Gaussian peaks. The fractions of Na–O– ^{4}Si /total NBO from the above methods decrease with increasing Ca content and are 43 (± 3)% (CNS051560), 18.2 (± 1)% (CNS116), and 4.1 (± 0.5)% (CNS150560), respectively.

For comparison we also obtained the fraction of Na–O– ^{4}Si from the ^{17}O MAS data at 9.4 T by fitting each spectrum based on the assumption of one BO site and four NBO sites (^4Na , $^2\text{Na}^1\text{Ca}$, $^1\text{Na}^2\text{Ca}$, ^3Ca), where each of the latter is further assumed to be a Gaussian function (Figure 7). The choice of types of NBO peaks is rather arbitrary (e.g., 3Na or 4Na for end members, or the existence of a $3\text{Na}^1\text{Ca}$ NBO peak, etc.), but the purpose of the fitting is to obtain a Na–O– ^{4}Si fraction that is represented by a rather well defined peak at about 25 ppm. Here we used five Gaussian functions (GAs) for BOs to map out the nonsymmetric peak shapes that are caused by the SQI as shown for the BO line shape in Figure 7. The five GAs for BOs for intermediate compositions are also assumed to vary with composition (Ca/Na ratio), which can account for the composition-dependent peak shape and can solve the problem of imperfect simulations of BO peak shapes that generally occur when using single mean values of δ_{iso} , C_q , and η . The

uncertainty in the Na—O—^[4]Si fraction is thus reduced. The series of spectra for intermediate compositions were fitted “individually” using five GAs for BOs and four GAs for NBOs (³Ca—O—^[4]Si, ²Ca¹Na—O—^[4]Si, ¹Ca²Na—O—^[4]Si, and ⁴Na—O—^[4]Si) where the fitting parameters (width and peak position) for Ca—O—^[4]Si from CS46 and simulation parameters (width and peak position) for Na—O—^[4]Si from the NS13 were used to constrain the fitting of the MAS NMR spectra with areas of Na—O—^[4]Si peak as fitting parameters. To examine the validity of the obtained Na—O—^[4]Si fractions from individual fitting and to obtain the constraints on mixed peaks and total NBO concentration, the spectra for intermediate compositions were then fitted “simultaneously” with area, width, and peak position of each mixed peaks, and area of Na—O—^[4]Si and Ca—O—^[4]Si as unknown fitting parameters. The total fraction of NBO in NS13 that is predicted from the composition is 28.6%, and those fractions obtained from fitting of NS13, CNS051560, CNS116, and CNS150560, are 26.4, 30.6, 24.4, and 29.5%, respectively. We consider this to be relatively good agreement and a successful test of this approach to the data analysis.

Figure 7 shows the fitting results for CNS116 and CNS051560. The source of error in this approach mostly stems from overlap between peaks for Na—O—Si and BO. The Na—O—^[4]Si/total NBO from this analysis is 38.6 (±2) (CNS051560), 12.8 (±2) (CNS116), and 4.4 (±1)% (CNS150560), respectively. The differences between the MAS and 3QMAS results are probably due to slightly different MQMAS efficiencies and to uncertainties associated with fitting different data sets. These values, particularly for CNS051560 and CNS116, are well constrained and thus can be compared with modeling. The Na—O—^[4]Si fractions for these samples are clearly much smaller than those predicted from random distributions of Na—Ca around NBO assuming either three (^MNa^NCa, where $M + N = 3$) or four possible configurations of network modifying cations around the NBO. For CNS051560 and CNS116, respectively, predictions are about 66.7% and 32.6% for the former ($M + N = 3$) and 54% and 19.8% for the latter ($M + N = 4$). The configuration used for fitting with an assumption of random distribution leads to 66.3% and 27.5% Na—O—^[4]Si for these two compositions.

All of these predicted values are larger than the experimental fraction of Na—O—^[4]Si, which indicates that Na—Ca distribution certainly deviates from a random distribution, with preference for Na—Ca pairing around NBOs. Another possible interpretation is that the smaller Na—O—^[4]Si fraction could stem from stronger interaction between Ca and NBO and hence “excess” Ca—NBO over the random case, but further analysis of this effect is more difficult to perform than for the Na—O—^[4]Si fraction alone, and the results can be model dependent. On the other hand, the results from ²³Na NMR also support the preference of dissimilar pairs.

Discussion

Structure of Mixed Cation Silicate Glasses and Degree of Intermixing among Charge-Modifying Cations. Implications for the “Mixed Cation Effect”. We have shown that there is strong tendency for the formation of dissimilar cation (Na—Ca) pairs in soda lime silicate glasses. This rather unusual preference may primarily stem from the difference in charges of these cations, given the similarity of their radii. The extent of cation mixing in various silicate glasses may differ significantly depending on the ionic radii and charges of the cations as well as different medium-range order in the melts; this further complicates the extent of disorder. Strong preference for certain

arrangements of network-modifying cations has been found in our recent study on Ba—Mg silicate glasses, where Ba and Mg tend to show chemical order around NBO forming only ³Ba—O—^[4]Si and ¹Ba²Mg—O—^[4]Si in BaMgSi₂O₆ glass and Ba also shows further preferential proximity to both NBO and BO compared with Mg (Lee et al., in review). This kind of strong preference among network-modifying cations as well as between network-modifying cations and frameworks is probably caused by a large difference in ionic radii (Mg²⁺, 0.72 Å; Ba²⁺, 1.35 Å) as previously reported in K—Mg silicate glasses.¹⁴ This strong ordering or preference to certain types of oxygen sites is not shown either in the Ca—Na silicates or in the previously studied Ca—Mg system,¹³ possibly due to similar ionic radii (Na⁺, 1.02; Ca²⁺, 0.99). Larger differences in ionic radii increase the site mismatch energy, which may contribute to strong ordering around NBO. The charge difference apparently plays an important role in the preference to the formation of dissimilar pairs primarily in order to maximize a homogeneous distribution of charges in the glasses.

Another salient result from this study is the evidence of interactions of framework cations and anions with network-modifying cations. Recently we proposed a “perturbed Na distribution model” in silicate glasses based on ²³Na NMR at high field, in which nonframework cations are homogeneously distributed and thus probes the types of NBO or BOs determined by composition and the degree of network disorder, but the distance between nonframework cations and network units (BO and NBO) reflect their relative affinity (e.g., stronger interactions between Na and NBO over BO). The results given here also support the model.

Nonrandom distributions of modifying cations in Ca—Na silicate glasses will affect the dynamics of Na⁺ and related transport properties in the glass and melt, although as-yet unknown effects of temperature will need to be assessed before extrapolating structural data on these glasses to temperatures much above the glass transition. One such intriguing effect, the slowing down of Na⁺ ion mobility with increasing Ca content, was also noted in molecular dynamics simulations.⁸ To explain these mixed cations effects, it has been suggested that it is more difficult for a cation to hop to a site previously occupied by another type of cation than to a site vacated by the same type of cation.¹¹ Upon mixing among network-modifying cations, the number of Na neighbors to Na decrease from the pure systems reducing energetically favorable sites for ionic hopping, which is also the case for a random distribution of cations with effectively fewer Na—Na pairs than those in single cation silicate glasses. The available sites for hopping can further decrease with increasing prevalence for dissimilar pairs. Thus the experimental results from this study, showing extensive mixing of dissimilar cations with a preference for Na—Ca pairing, can partly account for a decrease in diffusivity upon mixing. The experimental activation energy barrier (in the temperature range 1123–1473 K) of Na⁺ diffusion in Ca—Na silicate glasses (CaO/Na₂O/SiO₂ = 1:1:4) is larger (19.9 kcal/mol) than that in K—Na silicate glasses (K₂O/Na₂O/SiO₂ = 1:1:4) glass (16.1 kcal/mol) even with less actual concentration of Ca for the former, while the activation energy barrier for Na⁺ of binary sodium disilicates glasses (Na₂O/SiO₂=1:2) is 11.9 kcal/mol.³⁵ The K—Na silicate system has been reported to show a random Na—K distribution and thus has a higher probability of having Na neighbors to Na sites. This trend in activation energies thus supports our atomistic interpretation of preference to dissimilar pairs in the Na—Ca system.

Implications on Transport and Thermodynamic Properties of Silicate Melts and Magmas. The diffusivity of Na and its relationship to the effects of composition on melt structure plays a key role in melt properties. The results given here provide important constraints on models of the mobility of cations in silicate glasses and the corresponding liquids as discussed above. Nonrandom distributions of Na–Ca, and further preference for dissimilar pairs, can contribute negatively to the configurational entropy from mixing of these cations, possibly contributing to an increase in the viscosity of silicate melts over that predicted from a random distribution.^{1–5}

Partial cation ordering in the Ca–Na silicate system may also affect the silica activity of melts, and thus the phase equilibria during partial melting of peridotite in the earth's mantle (Lee et al., in preparation). Nonrandomness in the melts, together with extensive mixing in framework units, may strongly affect the melt composition that is produced, causing the alkali or silica content to increase when in equilibrium with mantle peridotite, as shown in silica-rich inclusions in mantle xenoliths³⁶ and in recent experiments.²³ The extent of nonrandomness in the system is likely to decrease with increasing temperature. The possibility of finding similar types of cations increases, and thus the hopping probability increases; this will contribute to the observation that the mixed cation effect decreases with increasing temperature.¹² The results given here suggest that the clear deviation from random distribution of different cations in Ca–Na silicate glasses and the nonrandomness associated with interaction among framework cations can both contribute to several transport properties of basaltic magmas and can also provide atomic-level constraints on models of mantle melting and configurational thermodynamic properties, including silica activity, manifesting the strong links between melt structures, properties, and magmatic processes.

Conclusion

Despite the ubiquity of soda-lime silica glass in technological applications and the importance of the system as a model for silicate magmas, in particular for peridotite melts, the extent of atomic disorder in cation distributions was not fully understood. Here we quantified the extent of intermixing among network-modifying cations in Ca–Na silicate glasses using ¹⁷O MAS NMR, 3QMAS NMR, and ²³Na MAS NMR spectra. These clearly demonstrate the prevalence of Na–Ca pairs and provide evidence of interaction among network-modifying cations and bridging oxygens as well as nonbridging oxygens. These results are contrary to models of glass structure favoring segregations of alkali or alkaline earth cations mainly surrounded by nonbridging oxygens. The preference for dissimilar pairs plays an important role in the strong compositional dependence of transport properties of glasses and melts, including Na diffusivity decrease with Ca content, and can support a negative deviation in silica activity that has strong implications to mantle melting. The extent of intermixing of cations in several mixed cation silicate glasses shows strong deviation from nonrandomness and

appears to be primarily governed by charge and ionic radii differences among cations.

Acknowledgment. This project was supported by a Stanford Graduate Fellowship and a Carnegie Postdoctoral Fellowship to Dr. Sung Keun Lee and by an NSF Grant EAR 0104926 to Professor Jonathan F. Stebbins. We also thank two anonymous reviewers for helpful comments.

References and Notes

- (1) Mysen, B. O.; Virgo, D.; Seifert, F. A. *Rev. Geophys. Space Phys.* **1982**, *20*, 353.
- (2) Navrotsky, A.; Peraudeau; McMillan, P.; Coutures, J. P. *Geochim. Cosmochim. Acta* **1982**, *46*, 2039.
- (3) Toplis, M. J.; Dingwell, D. B.; Hess, K.; Lency, T. *Am. Mineral.* **1997**, *82*, 979.
- (4) Lee, S. K.; Stebbins, J. F. *Am. Mineral.* **1999**, *84*, 937.
- (5) Lee, S. K.; Stebbins, J. F. *J. Non-Cryst. Solids* **2000**, *270*, 260.
- (6) Gee, B.; Eckert, H. J. *Phys. Chem.* **1996**, *100*, 3705.
- (7) Vessal, B.; Greaves, G. N.; Marten, P. T.; Chadwick, A. V.; Mole, R.; Houdewalter, S. *Nature* **1992**, *356*, 504.
- (8) Cormack, A. N.; Cao, Y. *Mol. Eng.* **1996**, *6*, 183.
- (9) Yap, A. T. W.; Forster, H.; Elliott, S. R. *Phys. Rev. Lett.* **1995**, *75*, 3946.
- (10) Bray, P. J.; Emerson, J. F.; Lee, D.; Feller, S. A.; Bain, D. L.; Feil, D. A. *J. Non-Cryst. Solids* **1991**, *129*, 240.
- (11) Maass, P.; Bunde, A.; Ingram, M. D. *Phys. Rev. Lett.* **1992**, *68*, 3064.
- (12) Greaves, G. N. *Solid State Ionics* **1998**, *105*, 243.
- (13) Kirkpatrick, R. J. MAS NMR spectroscopy of minerals and glasses. In *Spectroscopic Methods in Mineralogy and Geology*; Hawthorne, F. C., Ed.; Mineralogical Society of America: Washington DC, 1988; p 341.
- (14) Farnan, I.; Grandinetti, P. J.; Baltisberger, J. H.; Stebbins, J. F.; Werner, U.; Eastman, M.; Pines, A. *Nature* **1992**, *358*, 31.
- (15) Florian, P.; Vermillion, K. E.; Grandinetti, P. J.; Farnan, I.; Stebbins, J. F. *J. Am. Chem. Soc.* **1996**, *118*, 3493.
- (16) Stebbins, J. F.; Oglesby, J. V.; Xu, Z. *Am. Mineral.* **1997**, *82*, 1116.
- (17) Mueller, K. T.; Wu, Y.; Chmelka, B. F.; Stebbins, J.; Pines, A. *J. Am. Chem. Soc.* **1990**, *113*, 32.
- (18) Frydman, I.; Harwood: J. S. *J. Am. Chem. Soc.* **1995**, *117*, 5367.
- (19) Timken, H. K. C.; Schramm, S. E.; Kirkpatrick, R. J.; Oldfield, E. *J. Phys. Chem.* **1987**, *91*, 1054.
- (20) Bunker, B. C.; Tallant, D. R.; Kirkpatrick, R. J.; Turner, G. L. *Phys. Chem. Glasses* **1990**, *31*, 30.
- (21) Lee, S. K.; Stebbins, J. F. *J. Phys. Chem. B* **2000**, *104*, 4091.
- (22) Lee, S. K.; Stebbins, J. F. *Geochim. Cosmochim. Acta* **2002**, *66*, 303.
- (23) Hirschmann, M. M.; Baker, M. B.; Stolper, E. M. *Geochim. Cosmochim. Acta* **1998**, *62*, 883.
- (24) Kentgens, A. P. M.; Verhagen, R. *Chem. Phys. Lett.* **1999**, *300*, 435.
- (25) Vosegaard, T.; Massiot, D.; Grandinetti, P. J. *Chem. Phys. Lett.* **2000**, *326*, 454.
- (26) Zhao, P.; Neuhoff, P. S.; Stebbins, J. F. *Chem. Phys. Lett.* **2001**, *344*, 325.
- (27) Lee, S. K.; Stebbins, J. F. *Geochim. Cosmochim. Acta*, in press.
- (28) Lee, S. K.; Stebbins, J. F. *Am. Mineral.* **2003**, *88*, 493.
- (29) Baltisberger, J. H.; Xu, Z.; Stebbins, J. F.; Wang, S.; Pines, A. *J. Am. Chem. Soc.* **1996**, *118*, 7209.
- (30) Grandinetti, P. J.; Baltisberger, J. H.; Farnan, I.; Stebbins, J. F.; Werner, U.; Pines, A. *J. Phys. Chem.* **1995**, *99*, 12341.
- (31) Amoureux, J. P.; Fernandez, C.; Frydman, L. *Chem. Phys. Lett.* **1996**, *259*, 347.
- (32) Medek, A.; Harwood: J. S.; Frydman, L. *J. Am. Chem. Soc.* **1995**, *117*, 12779.
- (33) Xue, X.; Stebbins, J. F. Kanzaki, M. *Am. Mineral.* **1994**, *79*, 31.
- (34) Stebbins. *Solid State. Ionics* **1998**, *112*, 137.
- (35) Malkin, V. I.; Mogutnov, B. M. *Dokl. Akad. Nauk SSSR* **1961**, *141*, 1127.
- (36) Lundstrom, C. C. *Nature* **2000**, *403*, 527.